Synthesis of Mesocellular Silica Foams with Tunable Window and Cell Dimensions

Wayne W. Lukens, Jr., Peidong Yang, and Galen D. Stucky*

Department of Chemistry and Materials Research Laboratory, University of California, Santa Barbara, California 93106

Received July 29, 1999. Revised Manuscript Received May 2, 2000

Polystyrene microspheres coated with cationic surfactants are easily prepared by microemulsion polymerization. These microspheres can be used in place of surfactants to synthesize porous silica foams. The nature of the foams depends strongly upon the synthesis conditions. Under basic catalysis, "closed-cell" foams are obtained. Under acidic catalysis, open-cell foams are obtained. The windows that connect the cells of the open-cell foams are believed to arise from direct contact between adjacent spherical templates. These silica foams resemble dense aerogels.

Introduction

Because of their greatly enhanced pore diameters,[1] mesoporous materials with well-defined pore structures have received increasing attention as potential catalysts[2] and as supports for catalysis[3] and separations.[4] Because the utility of these materials is largely due to the structure and size of their pores, a number of strategies have been developed for controlling the size, shape, and connectivity of the pore systems in these materials. Most of these strategies rely upon replicating surfactant phases with silica, presumably through the intermediacy of a silicate−surfactant liquid crystal phase. The Mobil group reported the best-known examples, namely, MCM-41, MCM-48, and MCM-50, which are analogues of hexagonal *p*6*mm*, cubic *Ia*3*d*, and lamellar liquid crystal phases, respectively.[1b,c] Huo et al. demonstrated that changing the surfactant packing parameter in a rational manner allows the synthesis of new silica mesostructures.[5] Attard and Pinnavaia and co-workers used nonionic surfactants to synthesize materials with cylindrical pores and considerable textural mesoporosity due to pores formed between the relatively small particles.[6] Zhao and others showed that block-copolymer surfactants together with an organic cosolvent can be used to expand the pore size of the *p*6*mm* materials to greater than 250 Å.[7] The use of emulsion biphasic chemistry in materials synthesis has demonstrated the simultaneous control of particle shape on the micrometer to centimeter length scale and of the periodic mesostructure at the molecular scale (15−100 Å).[8] The final morphology produced by this chemistry can be determined using shear flow to produce, for example, hollow spheres with diameters of 1−100 μm. McGrath et al. reported templating of silica by the L_3 "sponge phase".[9]

Except for the sponge phase, in all of these approaches, the dimensions of the mesopores in the materials are dictated by the dimensions of the micelles. More recently, colloidal templates have produced materials with larger pores. The use of emulsion-polymerized polystyrene as a template for silica with 0.2−1 μm pores has been reported.[10] Yang et al. used emulsion-polymerized polystyrene to produce porous materials that are ordered over multiple length scales.[11] Imhof and Pine synthesized a number of porous oxides with pore sizes ranging from 50 nm to 5 μm using coalesced, fractionated emulsions as templates.[12] Antonietti and co-workers synthesized silica with pores ranging in size from 20 to 200 nm using functionalized polymers, including microemulsion-polymerized polystyrene, as templates.[13] Schmidt-Winkel et al. used microemulsions

* Address correspondence to this author at: Department of Chemistry, University of California, Santa Barbara, CA 93106, stucky@chem.ucsb.edu.

(1) (a) Yanagisawa, T.; Shimizu, T.; Kuroda, K.; Kato, C. *Bull. Chem. Soc. Japan* **1990**, *63*, 988. (b) Kresge, C. T.; Leonowicz, M. E.; Roth, W. J.; Vartuli, J. C.; Beck, J. S. *Nature* **1992**, *359*, 710. (c) Beck, J. S.; Vartuli, J. C.; Roth, W. J.; Leonowicz, M. E.; Kresge, C. T.; Schmitt, K. D.; Chu, C. T.-W.; Olsen, D. H.; Sheppard, E. W.; McCuller, S. B.; Higgins, J. B.; Schlenker, J. L. *J. Am. Chem. Soc.* **1992**, *114*, 10834. (d) Inagaki, S.; Fukushima, Y.; Kuroda, K. *J. Chem. Soc., Chem. Commun.* **1993**, 680.

(2) (a) Blasco, T.; Corma, A.; Navarro, M. T.; Pérez Pariente, J. *J. Catal.* **1995**, *156*, 65. (b) Gontier, S.; Tuel, A. *Zeolites* **1995**, *15*, 601. (c) Zhang, W.; Wang, J.; Tanev, P. T.; Pinnavaia, T. J. *Chem. Commun.* **1996**, 979.

(3) (a) Maschmeyer, T.; Rey, F.; Sankar, G.; Thomas, J. M. *Nature* **1995**, *378*, 159. (b) Burch, R.; Cruise, N.; Gleeson, D.; Tsang, S. C. *Chem. Commun.* **1996**, 951. (c) Walker, J. V.; Morey, M.; Carlsson, H.; Davidson, A.; Stucky, G. D.; Butler, A. *J. Am. Chem. Soc.* **1997**, *119*, 6921.

(4) (a) Feng, X.; Fryxell, G. E.; Wang, L.-Q.; Kim, A. Y.; Liu, J.; Kemner, K. M. *Science* **1997**, *276*, 923. (b) Mercier, L.; Pinnavaia, T. J. *Adv. Mater.* **1997**, *9*, 500.

(5) Huo, Q.; Leon, R.; Petroff, P. M.; Stucky, G. D. *Science* **1995**, *268*, 1324.

(6) (a) Tanev, P. T.; Pinnavaia, T. J. *Science* **1995**, *267*, 865. (b) Bagshaw, S. A.; Prouzet, E.; Pinnavaia, T. J. *Science* **1995**, *269*, 1242. (c) Attard, G. S.; Glyde, J. C.; Göltner, C. G. *Nature* **1995**, *378*, 366.

(7) Zhao, D.; Feng, J.; Huo, Q.; Melosh, N.; Fredrickson, G. H.; Chmelka, B. F.; Stucky, G. D. *Science* **1998**, *279*, 548.

(8) Schacht, S.; Huo, Q.; Voight-Martin, I. G.; Stucky, G. D.; Schüth, F. *Science* **1998**, *273*, 768.

(9) McGrath, K. M.; Dabbs, D. M.; Yao, N.; Aksay, I. A.; Gruner, S. M. *Science* **1997**, *277*, 552.

(10) (a) Holland, B. T.; Blanford, C. F.; Stein, A. *Science* **1998**, *281*, 538. (b) Velev, O. D.; Jede, T. A.; Lobo, R. F.; Lenhoff, A. M. *Nature* **1997**, *389*, 447.

(11) Yang, P.; Deng, T.; Zhao, D.; Feng, P.; Pine, D.; Chmelka, B. F.; Whitesides, G. M.; Stucky, G. D. *Science* **1998**, *282*, 244.

(12) (a) Imhof, A.; Pine, D. J. *Nature* **1997**, *389*, 948. (b) Imhof, A.; Pine, D. J. *Adv. Mater.* **1998**, *10*, 697. (c) Imhof, A.; Pine, D. J. *Adv. Mater.* **1999**, *11*, 311.

10.1021/cm991109c CCC: $20.00
Published on Web 01/15/2001

to template mesocellular silica foams with pore diameters ranging from 22 to 36 nm.[14] Although all of these methods generally produce materials with well-defined, spherical pores, the macroporous materials have much lower surface areas than the mesoporous materials. In addition, apart from microemulsions and microemulsion-polymerized polystyrene, the colloidal templates are either difficult or time-consuming to prepare.

We were interested in using microemulsion-polymerized polystyrene as a template for two reasons. It is easy to prepare, and polystyrene microspheres coated with cationic surfactants[15] (cationic microspheres) are similar to the mesitylene swollen micelles of the Mobil group's solvent-expanded MCM-41 synthesis.[1c] This analogy suggests that cationic microspheres can be employed in the MCM-41[1] (basic conditions) or SBA-3[16] (acidic conditions) syntheses in lieu of cosolvent-swollen surfactant micelles. However, rather than producing silica with cylindrical pores, the spherical template should produce silica foams with large spherical cells (templated by the microspheres) connected by smaller windows. In this paper, we describe the silica foams produced using microemulsion-polymerized polystyrene as a template under various synthesis conditions.

Experimental Section

Measurements. Dynamic light-scattering measurements were performed using a Brookhaven Instruments light-scattering goniometer. Data were obtained at 3−5 angles between 60° and 135°. Particle size and size distribution information was obtained from the autocorrelation function both by the second cumulant method and by nonnegatively constrained least-squares fitting of the autocorrelation function.[17] Gas adsorption data were obtained using a Micromeritics ASAP-2000 porosimeter. BET surface area determinations were performed over a relative pressure range of 0.05−0.16, and 13.5 Å^2 was used as the molecular area for nitrogen adsorbed on silica.[18] Pore size distributions were determined using a variation of the Broekhoff−de Boer method by using Hill's approximation to calculate the thickness of the adsorbed gas layer.[19] Scanning electron microscopy (SEM) was performed with a JEOL-6300F instrument equipped with a field-emission electron gun operating with an accelerating voltage of 3 kV. Samples were deposited from acetone suspension onto aluminum stubs and sputter-coated with ca. 100 Å of gold−palladium. Transmission electron microscopy (TEM) was performed using a JEOL-2000FX microscope operating at 200 kV. Samples were deposited from an acetone suspension onto Formvar coated copper grids. Simultaneous thermogravimetric and differential thermal analyses were performed on a Netzsch STA-409 instrument.

Syntheses. The inhibitors in commercially available styrene were removed either by washing the styrene with 10% sodium hydroxide or by passing it through a column of basic alumina. Water was deionized. All other reagents were used as received. Typical syntheses are reported here.

Representative Polystyrene Polymerizations in Microemulsion. (a) Nonionic Radical Initiator. A solution of 1,1′-azobis(cyclohexanecarbonitrile) (0.10 g, 0.41 mmol), styrene (30 mL, 27 g, 260 mmol), and 1,3-diisopropenylbenzene (2.5 mL, 2.3 g, 14 mmol) was slowly added to a magnetically stirred solution of hexadecyltrimethylammonium chloride (CTAC, 10 g, 31 mmol) in 90 mL of water. The milky white mixture was degassed under vacuum, placed under argon, and heated to 70 °C for 12 h in an oil bath. After this time, the solution scattered light less strongly but was still white.

(b) Potassium Persulfate Plus N,N,N′,N′-Tetramethyldiaminomethane (Anionic Radical Initiator).[19] A mixture of styrene (43 mL, 39 g, 380 mmol) and 1,3-diisopropenylbenzene (0.9 mL, 0.8 g, 5 mmol) was slowly added to a magnetically stirred solution of hexadecyltrimethylammonium chloride (CTAC, 10 g, 31 mmol) in 80 mL of water. The milky white solution was degassed under vacuum and placed under argon. *N,N,N′,N′*-tetramethyldiaminomethane (0.5 mL, 0.4 g, 4 mmol), followed by a solution of potassium persulfate (0.52 g, 1.9 mmol) in 10 mL of water, was added to the reaction mixture. The solution quickly became warm and was more translucent after ca. 15 min. The mixture was stirred for at least 2 h.

(c) Cationic Radical Initiator. A mixture of styrene (44 mL, 40 g, 380 mmol) and 1,3-diisopropenylbenzene (1.3 mL, 1.2 g, 7.7 mmol) was slowly added to a magnetically stirred solution of hexadecyltrimethylammonium chloride (CTAC, 10 g, 31 mmol) in 80 mL of water. The milky white mixture was degassed under vacuum, placed under argon, and heated to 70 °C with a water bath. A solution of 2,2′-azobis(2-methylpropionamidine) dihydrochloride (0.52 g, 1.9 mmol) dissolved 10 mL of water was added quickly to the reaction mixture, and the mixture was degassed under vacuum and placed under argon. After ca. 15 min, the reaction mixture was more translucent. The mixture was stirred at 70 °C for at least 2 h.

Representative Silica Mesofoam Syntheses. Silica foams were prepared by three different methods: those using basic conditions, acidic conditions, and sol−gel conditions. Basic conditions are similar to those used in the MCM-41 synthesis.[1b,c] Acidic conditions are similar to those used in the SBA-3 synthesis.[16b] Syntheses under sol−gel conditions are also performed in acid, but the tetraethyl orthosilicate (TEOS) is first hydrolyzed and partially polymerized and the mixture is allowed to gel after the addition of the template. The sol−gel conditions are similar to those described by Antonietti and coworkers.[13] Finally, both the synthesis in base and synthesis in acid were performed as "one-pot" syntheses in which the emulsion polymerization and silica synthesis were performed sequentially in the same vessel.

Basic Conditions. To 29.2 mL of water was added 2 mL of aqueous sodium hydroxide (2 M, 4 mmol) and 8.8 mL of a solution of CTAC-coated polystyrene spheres (0.24 M in CTAC, 2.1 mmol of CTAC). The blue-white solution was stirred, and tetraethyl orthosilicate (TEOS, 4.8 mL, 4.5 g, 23 mmol) was added. A white precipitate appeared after ca. two minutes. The mixture was stirred for 12 h, and then filtered, washed with 3 × 20 mL of water, and dried on the filter; the yield was 3.6 g. A 1.00 g sample of this composite was calcined in air using the following conditions: temperature increasing from 25 to 500 °C over 4 h and then held at 500 °C for 6 h. The yield was 0.32 g, 32% based upon the initial mass.

Acidic Conditions. To 30 mL of aqueous hydrochloric acid (1 M, 30 mmol) was added 8.8 mL of a solution of CTAC-coated polystyrene spheres (0.24 M in CTAC, 2.1 mmol of CTAC). The blue-white solution was stirred, and tetraethyl orthosilicate (TEOS, 4.3 mL, 4.0 g, 19 mmol) was added. A white precipitate appeared after ca. 4 min. The mixture was stirred for 12 h, and then filtered, washed with 3 × 20 mL of water, and dried on the filter. The yield was 3.6 g. A 1.00 g sample of this composite was calcined in air using the following conditions: temperature increasing from 25 to 550 °C over 4 h and then held at 550 °C for 6 h. The yield was 0.22 g, 22% based upon the initial mass.

(13) Antonietti, M.; Berton, B.; Göltner, C.; Hentze, H.-P. *Adv. Mater.* **1998**, *10*, 154.
(14) Schmidt-Winkel, P.; Lukens, W. W.; Zhao, D. Y.; Yang, P. D.; Chmelka, B. F.; Stucky, G. D. *J. Am. Chem. Soc.* **1999**, *121*, 254.
(15) Antonietti, M.; Bremser, W.; Müschenborn, D.; Rosenauer, C.; Schupp, B. *Macromolecules* **1991**, *24*, 6636.
(16) (a) Huo, Q.; Margolese, D. I.; Ciesla, U.; Feng, P.; Gier, T. E.; Sieger, P.; Leon, R.; Petroff, P. M.; Schüth, F.; Stucky, G. D. *Nature* **1994**, *368*, 317. (b) Huo, Q.; Margolese, D. I.; Ciesla, U.; Demuth, D. G.; Feng, P.; Gier, T. E.; Sieger, P.; Firouzi, A.; Chmelka, B. F.; Schüth, F.; Stucky, G. D. *Chem. Mater.* **1994**, *6*, 1176.
(17) Morrison, I. D.;. Grabowski, E. F. *Langmuir* **1985**, *1*, 496.
(18) Jelinek, L.; sz. Kovátz, E. *Langmuir* **1994**, *10*, 4225
(19) (a) Lukens . W., Jr.; Schmidt-Winkel, P.; Zhao, D.; Feng, J.; Stucky, G. D. *Langmuir* **1999**, *15*, 5403. (b) Broekhoff, J. C. P.; de Boer, J. H. *J. Catal.* **1967**, *9*, 15. (c) Hill, T. L. *Adv. Catal.* **1952**, *4*, 211.

Table 1. Effect of Initiator and the Ratio of Styrene to Surfactant on the Size and Size Distribution of Microemulsion-Polymerized Polystyrene Spheres

radical initiator	[CTAC] (M)	styrene/CTAC wt ratio	initiator/styrene mol ratio (%)	diameter (2nd cum.)[a] (nm)	variance (2nd cum.)[a]	diameter (NNLS)[b] (nm)	variance (NNLS)[b]
nonionic	0.31	1/3	1.4	29.5	0.19	–	–
nonionic	0.31	1/1	0.2	40.4	0.13	–	–
nonionic	0.31	3/1	0.2	52.2	0.19	–	–
anionic	0.33	1/2	1.9	22.9	0.19	21.7	0.04
anionic	0.33	1/1	1.9	27.4	0.10	27.0	0.05
anionic	0.33	3/1	1.9	31.1	0.10	31.0	0.01
anionic	0.08	2/1	1.0	37.9	0.15	36.7	0.01
anionic	0.08	2/1	2.0	33.8	0.19	34.3	0.01
anionic	0.08	2/1	4.0	29.4	0.20	29.2	0.01
cationic	0.31	4/1	0.5	35.3	0.09	34.3	0.01
cationic	0.06	2/1	1.0	35.0	0.08	36.0	<0.01
cationic	0.06	4/1	0.5	47.3	0.08	48.0	0.01
cationic	0.06	6/1	0.3	54.5	0.04	53.3	<0.01

[a] Particle size and size distribution determined by the second cumulant method. [b] Particle size and size distribution determined by nonnegatively constrained least-squares analysis of the autocorrelation function.[17]

Sol−Gel Conditions. Aqueous hydrochloric acid (15 mL, 0.03 M, 0.5 mmol) was heated to 60 °C. To the rapidly stirring solution was added TEOS (1.8 mL, 1.7 g, 6 mmol), and the mixture was stirred for 1 h, forming a slightly cloudy solution. To the rapidly stirred solution was added 5 mL of a solution of CTAC-coated polystyrene spheres (0.24M in CTAC, 1.2 mmol of CTAC). The mixture was poured into a Petri dish and covered. The Petri dish was placed in a 60 °C oven for 7 days, during which time the mixture formed a translucent gel. The Petri dish was then uncovered, and the gel was dried at 60 °C. The gel cracked into 0.5−2 mm chunks; the yield was 2.00 g. A 0.52 g sample of this composite was calcined in air using the following conditions: temperature increasing from 25 to 550 °C over 4 h and then held at 550 °C for 6 h. The calcined material had roughly the same translucency or transparency as the uncalcined xerogel; the yield was 0.097 g, 19% based upon the initial mass.

One-Pot Synthesis of Silica Mesofoam. A solution of CTAC (2.0 g, 6.3 mmol) in 93 mL of water was heated to 60 °C, and styrene (8.8 mL, 8.0 g, 77 mmol) and 1,3-diisopropenylbenzene (0.10 mL, 0.09 g, 0.6 mmol) were added. The mixture was degassed and placed under argon. A solution of 2,2′-azobis(2-methylpropionamidine) dihydrochloride (0.10 g, 0.4 mmol) dissolved in 5 mL of water was added quickly, and the mixture was again degassed under vacuum and placed under argon. After ca. 15 min, the solution became translucent and bluish. After the solution was stirred for 12 h, sodium hydroxide (5M in water, 2.0 mL, 10 mmol) or concentrated hydrochloric acid (2.0 mL, 24 mmol) was added, followed by TEOS (14 mL, 13 g, 63 mmol). White precipitate appeared in 2 min under basic conditions or 2 h under acidic conditions. The mixture was stirred for another 12 h, and then filtered and washed with 100 mL of water. The white solid was dried on the filter. The yield was 13.3 g, for synthesis in base. A 1.00 g sample of this composite was calcined in air using the following conditions: temperature increasing from 25 to 550 °C over 4 h and then held at 550 °C for 6 h. The yield was 0.29 g, 29% based upon the initial mass, for the basic synthesis.

Results

Template Synthesis. Because we used the polystyrene microspheres as templates, we were mainly interested in the reproducibility of the synthesis and the size and size distribution of the resulting particles. We examined three different radical initiators: nonionic, 1,1′-azobiscyclohexanecarbonitrile; anionic, potassium persulfate plus *N*,*N*,*N*′,*N*′-tetramethyldiaminomethane;[20] and cationic, 2,2′-azobis(2-methylpropionamidine) dihydrochloride. Results for the different initiators and varying ratios of styrene to surfactant are given in Table 1. The size of the microspheres obtained depended upon the styrene-to-surfactant ratio, the concentration of surfactant, and the styrene-to-initiator ratio. Whereas the size of the microspheres varied in response to the reaction conditions, independent syntheses with identical parameters produced microspheres with very similar sizes and size distributions when either the cationic or the anionic radical initiators were used. Syntheses using the nonionic radical initiator were less reproducible. In addition, for a given styrene-to-surfactant ratio, the nonionic radical initiator usually produced larger particles than either of the other initiators. Because of the decreased specific surface area of the larger particles, polymer solutions produced using the nonionic initiator usually had a considerable amount of free surfactant. This free surfactant acted as a template for cylindrical mesopores, producing an unwanted bimodal distribution of pore sizes in silica foams templated by these solutions. The foams with the bimodal pore distribution closely resemble those described by Antonietti et al., even though the templates and reaction conditions are quite different.[13]

The width of the size distribution of the microspheres is also a function of the synthesis conditions, as shown in Table 1. The cationic radical initiator generally produced microspheres with a smaller size distribution than either the nonionic or anionic radical initiators. However, in no case was the width of the size distribution small enough to produce ordered materials analogous to silica templated by colloidal crystals.[10]

Silica Foams. *Synthesis in Base.* The synthesis of silica foam under basic conditions is analogous to the synthesis of MCM-41.[1] The microemulsion polymerization and the silica/microsphere composite synthesis can be conveniently carried out in a one-pot synthesis, which is especially useful for preparing silica foams on a larger scale. Selected physical properties of silica foams synthesized under basic conditions are listed in Table 2. In all cases, the final silica-to-surfactant ratio (Si/N), determined from thermogravimetric analysis (TGA) using the weight ratio of surfactant to styrene, was very similar to the initial silica-to-surfactant ratio in the synthesis mixture. The large pore volumes and moderate surface areas of these foams are consistent with the presence of large mesopores whose walls are not microporous.

(20) (a) Larpent, C.; Bernard, E.; Richard, J.; Vaslin, S. *Macromolecules* **1997**, *30*, 354. (b) Roy, R.; Laferrière, C. A. *Carbohydr. Res.* **1988**, *177*, C1.

Table 2. Properties of Silica Mesocellular Foams Produced under Basic Conditions

sample	initial Si/N ratio[a]	wt % SiO_2 of composite	final Si/N ratio[a]	template diam (nm)	cell diam (nm)	window diam (nm)	pore volume ($cm^3\ g^{-1}$)	surface area ($m^2\ g^{-1}$)
I82	8.8	39	7.6	40	25	<5	1.1	558
I84	9.8	28	8.8	52	43	<5	1.7	483
VI54	10.0	27	10.4	47	45	<5	1.4	300
VI58	10.0	NM[b]	NM[b]	53	57	<5	2.2	375
VI77	7.7	30	7.2	36	35	<5	1.4	617

[a] Silica-to-surfactant ratio. [b] NM: not measured.

Scanning electron microscopy confirms the presence of large mesopores, as illustrated by the image of the silica foam shown in Figure 1a. A transmission electron microscope (TEM) image is shown in Figure 2a. Large mesopores are visible in the TEM image; however, no smaller pores are observed. The large pores appear to be separated by thin silica walls, and the overall structure consists of roughly spherical cells separated by thin silica walls. The material is reminiscent of clusters of soap bubbles and looks like a closed-cell foam.

Nitrogen adsorption measurements provide a slightly different view of the cell structure in these materials. A representative nitrogen adsorption isotherm and the pore size distribution derived from it are shown at the top of Figure 3. These materials have a type-IV isotherm with a type-H2 hysteresis loop.[21] The shapes of the isotherm and hysteresis loop suggest that these materials consist of large cells that are connected to each other and to the surface of the particle by much smaller windows.[22] The dimensions of the cells, determined from the adsorption branch of the isotherm, are reported in Table 1. In all cases, the dimensions of the cells are similar to the dimensions of the templates. In addition, templates with a wider size distribution produce a wider pore size distribution in the calcined materials.

Unlike the dimensions of the cells, the dimensions of the windows between the cells cannot be determined with certainty in these materials. All materials synthesized in base lose much of their adsorbed nitrogen at a relative pressure of 0.42−0.45. However, loss of nitrogen at this pressure at 77 K is not due to capillary evaporation but to the instability of the meniscus of the condensed nitrogen in the pores.[23] Below a relative pressure of 0.42, the gas and liquid in the pores always adopt the most thermodynamically favorable conformation. Although the windows between the cells must be smaller than 5 nm, the diameter of a cylindrical pore that undergoes capillary evaporation at this pressure, the size of the windows cannot be precisely determined from desorption of nitrogen at 77 K. The nitrogen

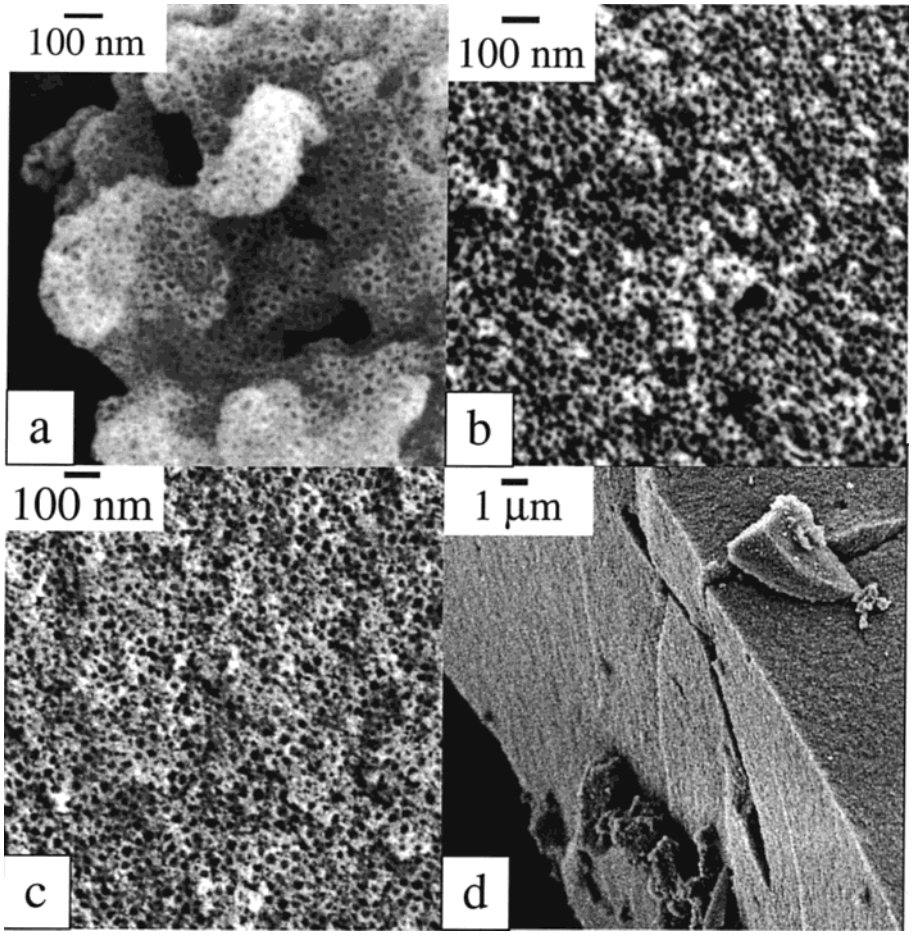

Figure 1. Scanning electron micrographs of silica foams: (a) synthesized in base, (b) synthesized in acid, (c) and (d) synthesized by the sol−gel route.

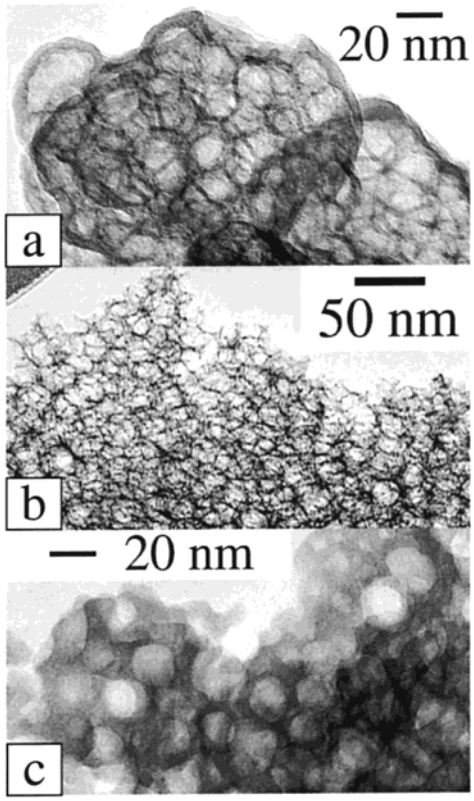

Figure 2. Transmission electron micrographs of silica foams: (a) synthesized in base, (b) synthesized in acid, (c) and (d) synthesized by the sol−gel route.

adsorption measurements suggest that these silica foams are not truly closed-cell foams, but open-cell foams in which the connecting windows are very much smaller than the cells. However, the physical structure of these foams, as determined by electron microscopy, is strongly reminiscent of closed-cell foam.

Synthesis in Acid. The synthesis of silica foam under acidic conditions is analogous to the synthesis of SBA-3.[24] As with the synthesis in base, the microemulsion polymerization and the silica/microsphere composite synthesis can be conveniently carried out as a one-pot reaction. Selected physical properties of these foams are listed in Table 3. Generally, these materials have larger specific pore volumes and specific surface areas than materials produced under basic conditions. Much of this difference is due to the lower silicon-to-surfactant ratio of the composite materials produced under acidic conditions. A significant amount of the silica introduced to the reaction mixture is not found in the composite material, so the materials produced under acidic conditions have thinner walls than analogous materials produced under basic conditions.

The cells in this material are visible in the SEM image shown in Figure 1b. The SEM images invariably show a closely packed, disordered array of pores in these materials. A typical TEM image is shown in Figure 2b. The TEM images also show closely packed pores, in agreement with the results from SEM. However, in marked contrast to the synthesis in base, the windows between the cells of this silica foam are clearly visible by TEM. The presence of the large windows between the cells suggests that this material is a spongelike, open-cell foam.

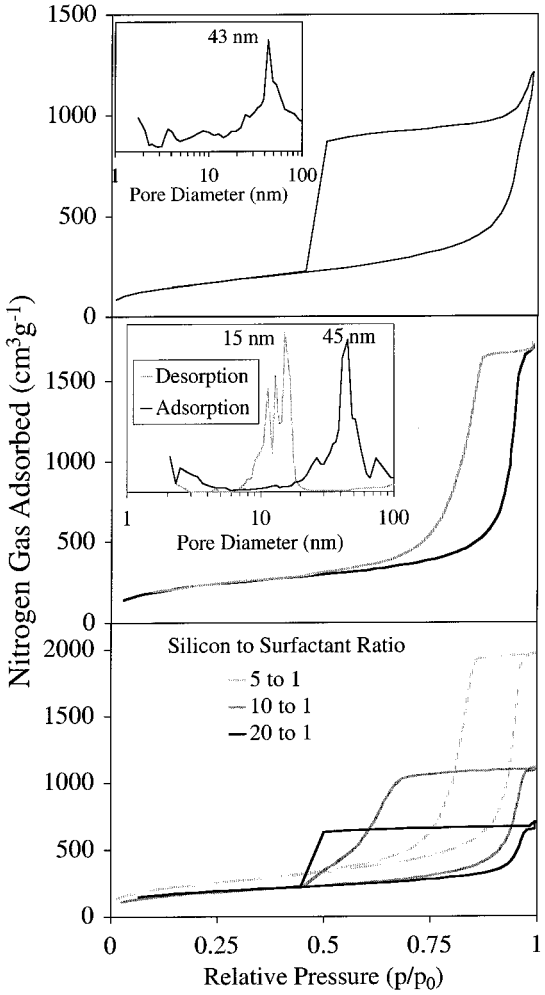

Figure 3. Nitrogen adsorption isotherms and pore size distributions (inset) of silica foams: top, synthesized in base; middle, synthesized in acid; bottom, synthesized by the sol−gel route with different silica-to-surfactant ratios. The spikes in the pore size distribution for the silica foam synthesized in acid are instrumental artifacts due to p_0 measurement.

This supposition is supported by gas adsorption measurements. An adsorption isotherm and the pore size distribution derived from it are shown in the middle of Figure 3. Like the materials synthesized in base, the cell sizes determined from the adsorption branch of the isotherm are in good agreement with the sizes of the templates used to make the materials. Unlike the materials synthesized in base, however, large windows connect the cells to each other and to the outside world, as shown by the pore size determined from the desorption branch of the isotherm. The size distributions of these windows are fairly narrow, similar to the size distributions of the cells. However, the windows are not similar in size to the templating microspheres or of the surfactant micelles.

(21) Sing, K. S. W.; Everett, D. H.; Haul, R. A. W.; Moscou, L.; Pierotti, R. A.; Rouquérol, J.; Siemieniewska, T. *Pure Appl. Chem.* **1985**, *57*, 603.

(22) Gregg, S. J.; Sing, K. S. W. *Adsorption, Surface Area and Porosity*; Academic Press: London, 1982.

(23) (a) Reference 22, pp 154ff. (b) Galarneau, A.; Desplantier, D.; Dutartre, R.; Di Renzo, F. *Microporous Mesoporous Mater.* **1999**, *27*, 297. (c) Inoue, S.; Hanzawa, Y.; Kaneko, K. *Langmuir* **1998**, *14*, 3079.

(24) A rhombic dodecahedron can be assembled from two identical cubes by slicing the second cube into six square pyramids and placing a pyramid on each face of the first cube. All formulas were derived using this relationship.

Table 3. Properties of Silica Mesocellular Foams Produced under Acidic Conditions

sample	initial Si/N ratio[a]	wt % SiO_2 of composite	final Si/N ratio[a]	template diam (nm)	cell diam (nm)	window diam (nm)	pore volume ($cm^3\ g^{-1}$)	surface area ($m^2\ g^{-1}$)
II7	9.1	24	6.7	52	43	14	2.5	942
II10	9.1	19	5.1	52	54	14	2.7	983
II11	9.1	NM[b]	NM[b]	52	48	11	3.2	995
VI55	10.0	20	7.3	48	45	15	2.7	696
VI59	10.0	NM[b]	NM[b]	56	86	19	3.2	545
VI78	7.7	24	5.2	36	32	7	2.0	854

[a] Silica-to-surfactant ratio. [b] NM: not measured.

Table 4. Properties of Silica Mesocellular Foams Produced under Sol−Gel Conditions

sample	initial Si/N ratio[a]	wt % SiO_2 of composite	final Si/N ratio[a]	template diam (nm)	cell diam (nm)	window diam (nm)	pore volume ($cm^3\ g^{-1}$)	surface area ($m^2\ g^{-1}$)
V111	5.2	14	4.5	53	54	14	3.2	721
V112	10.0	26	9.8	53	61	7	1.7	522
V113	20.0	39	18.9	53	60	<5	1.0	526
VI37	7.2	15	4.8	34	32	9	1.6	517
VI38	14.4	31	12.0	34	42	5	1.5	588
VI39	29.0	NM[b]	NM[b]	34	42	<5	1.0	560

[a] Silica-to-surfactant ratio. [b] NM: not measured.

Sol−Gel Synthesis. The silica foams obtained under sol−gel conditions closely resemble those obtained under acidic conditions with one major difference. Under sol−gel conditions, the ratio of silica to surfactant in the xerogel is the same as that in the synthesis mixture. Therefore, this ratio can easily be controlled by the synthesis conditions in contrast to the synthesis in acid.

The scanning electron micrographs of the silica foam prepared under sol−gel conditions are quite similar to those of the silica foam prepared in acid as shown in Figure 1c and 1d. The images show closely packed pores and are similar in appearance to images of materials synthesized in acid. A representative TEM image is shown in Figure 2c. In this image, the windows between the cells are readily apparent. Like the materials synthesized in acid, these materials appear to be open-cell foams.

The ratio of silica to surfactant has a pronounced effect upon the pore structures in these materials. The adsorption isotherms shown at the bottom of Figure 3 are for materials synthesized with the same template, but with different silica-to-surfactant ratios. The sizes of the cells are very similar as all of these materials undergo capillary condensation at the same relative pressure. However, the sizes of the windows vary greatly, as seen in the varying pressures of nitrogen loss in the desorption branches of the isotherms. Materials synthesized with a 20:1 silica-to-surfactant ratio had windows that were smaller than 5 nm, whereas materials synthesized with a ratio of 5:1 had 9 nm windows.

Discussion

The most surprising results of this study are the difference in pore structure between the materials synthesized in acid and in base and the presence of well-defined windows in materials synthesized under acidic conditions. Both of these effects are thought to result from the interactions between the template and the silica. Under basic conditions, the anionic silicate species interact strongly with the cationic template by the typical S^+I^- templating mechanism of MCM-41 type materials.[16b] Because of the strong interaction between the silica and the surfactant headgroup, the deprotonated silanol groups must remain in close proximity to the headgroup. Therefore, the entire surface of the template must remain covered by silica, although denser packings of silica and spheres may exist. Upon calcination, the silica shell remains largely intact, producing a material whose structure resembles a closed-cell foam.

These foams are not truly closed-cell foams, as is obvious from the fact that nitrogen can diffuse into the cells in the nitrogen adsorption experiments. Windows do connect the cells in these materials, but the windows are much smaller than cells, resulting in materials that look like closed-cell foams. Although the windows are presumably created during calcination by gases from the decomposing template, Antonietti and co-workers demonstrated that such windows can also result from surfactant micelles.[13] Because we were unable to determine either the window size or size distribution, we cannot suggest a mechanism for window formation in this case.

Under acidic conditions, the interaction between the silica and the template is most likely the $S^+X^-I^+$ mechanism of the SBA-1 and SBA-3 materials.[16b] In this case, the silanol groups are hydrogen-bonded to chloride ions associated with the cationic surfactant headgroups. Here, the interaction between the template and the silica is much weaker than the S^+I^- interaction, and the charge of the template is well screened by the chloride ions. Because the interaction between the silica and the template is weak, the silica and template can adopt a densely packed arrangement in which the template spheres are in contact. Calcination of the composite material produces open-cell foams that possess large windows, which may arise from the contact area between the spheres. These proposed mechanisms are shown in Scheme 1.

The premise that the windows are due to contact areas between the spheres suggests that the window size should be a function of the size of the template and the volume ratio of the silica and template. Qualitatively, this is true, as shown in the bottom plot of Figure 3 by the variation in window size with the silica-to-surfactant ratio. This relationship can also be examined more quantitatively by using a face-centered cubic (fcc) array of truncated spheres as a model for these disordered, but closely packed, silica foams.

Scheme 1. Proposed Mechanisms that Account for the Different Structures of the Silica Foams.

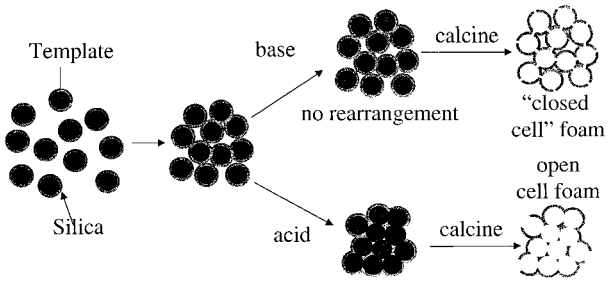

The building block of the model fcc foam is a sphere truncated by a rhombic dodecahedron (RD), shown in Figure 4. The volume of the RD is $4\sqrt{2}d^3$, where d is the distance from the center of a face to the center of the RD; the length of the edge of a face is $\sqrt{3/2}d$.[24] The volume of the truncated sphere is

$$\frac{4}{3}\pi(7r^3 + 3d^3 - 9dr^2)$$

where r is the radius of the sphere. The diameter of the window is $2\sqrt{r^2-d^2}$. If the truncated sphere is the template, whose radius is known from light scattering, and the volume of the silica is the remaining volume in the RD, then the volume ratio of silica to template is

$$\frac{4\sqrt{2}d^3}{\frac{4}{3}\pi(7r^3 + 3d^3 - 9dr^2)} - 1$$

By assuming that the density of the silica is 2.2 and the density of the template is 1.05, the volume ratio can be determined from thermal analysis, and the window diameter can be predicted. In Figure 5, the predicted window diameters are plotted against the window diameters determined from nitrogen adsorption. The measured values are, as expected, somewhat less than the predicted values, presumably because of the less than ideal truncated sphere geometry and packing observed in these disordered materials. However, despite the simplicity of the model, the observed and predicted window diameters are in good agreement, which supports the proposed mechanism for window formation.

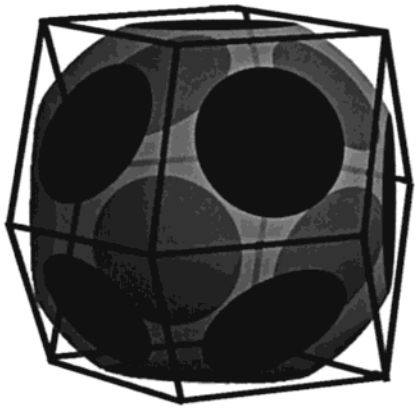

Figure 4. Sphere truncated by a rhombic dodecahedron, the building block of a model ordered foam with the fcc structure.

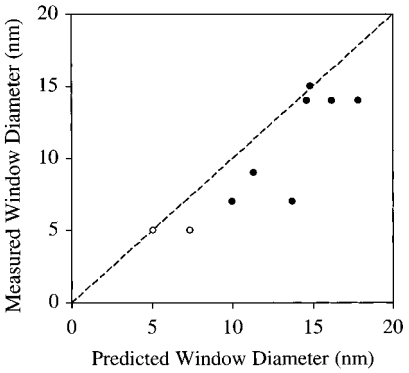

Figure 5. Comparison of the observed window diameter versus the window diameter predicted from the template size and the silica-to-template ratio using the fcc foam model. Open circles have measured pore diameters < 5 nm.

Because of their large pores and windows and very high surface areas and pore volumes, the silica foams prepared under acidic conditions are reminiscent of the more dense aerogels.[25] However, a number of differences exist between these silica foams and aerogels. The sphere templating route allows independent control of cell and window sizes. The cell size can be controlled by changing the template size, and the window size can be controlled by varying the silica-to-surfactant ratio. The sphere templating synthesis can easily and quickly be carried out as a one-pot synthesis, and supercritical drying is unnecessary to prepare these silica foams. Thus far, however, neither monolithic materials nor materials with very low density have been achievable by the sphere templating route.

Unlike the materials synthesized under acidic conditions, the materials synthesized under basic conditions do not resemble aerogels. Where the data is available, previously reported analogous materials, apart from titania foams reported by Imhof and Pine,[12c] resemble open-cell foams in which sizable windows connect the cells. Because the silica foam synthesized in base has smaller windows, passage of molecules through the bulk of the material should be more difficult than that through materials such as aerogels or silica foams synthesized in acid. Although the material looks like a very large pore material, it is not expected to behave like one. For this reason, this material is not expected to be a useful support for catalysis or separations; however, it should be a good thermal insulator and a good low-dielectric material.

Acknowledgment. This work was supported by NSF under Grants DMR-9520971 and DMR-9634396 and the U.S. Army Research Office under Grant DAAH04-96-2-0443. We thank Prof. David Pine for the use of the light-scattering goniometer. W.L. is grateful to the National Science Foundation for a Postdoctoral Fellowship. We made use of the UCSB Materials Research Laboratory Central Facilities supported by the NSF under Award DMR-9632716.

CM991109C

(25) Hüsing, N.; Schubert, U. *Angew. Chem., Int. Ed. Engl.* **1988**, *27*, 22.